QUANTIFYING AND DISCRITIZING THE UNCERTAINITY IN THE POWER PRODUCTION ESTIMATES OF A WAVE ENERGY CONVERTER

Helen Bailey[1], Bryson Robertson & Bradley Buckham
Mechanical Engineering Department,
University of Victoria, BC, Canada.

[1]Corresponding author: hlbailey@uvic.ca

INTRODUCTION

The ability to predictively assess Wave Energy Converter (WEC) power production is vital to the decision making process of WEC developers, electricity utilities and project financiers. However, when simulating a specific scenario there are numerous variables that introduce uncertainty in the prediction, even within a single seastate significant wave height (Hs) and energy period, (Te) bin. This work seeks to determine the causes of variability in mean power predictions and quantify the magnitude of these causes. The precise shape of the wave spectra and the exact values of Hs and Te are often not known, the random phases of the spectral constituents can never be predetermined, hydrodynamic parameters (i.e. viscous drag coefficients) may be in error and other environmental factors such as winds, currents and tidal heights are often omitted.

This work quantifies and discretizes the probability distributions (PD) of these variables and conducts a Monte Carlo experiment with over 12 000 high-fidelity simulation runs. All simulation runs and environmental factors are from within a single seastate bin. Each run models the dynamics of a 7 degree of freedom axisymmetric two body point absorber WEC. The PD of the 20-min mean WEC power is presented. The mean power is systematically detrended and the deterministic influence of each random variable is quantified through trend-based data fitting. The detrended mean power data reveals a baseline level of uncertainty in the mean power recovered; even with known model coefficients and environmental conditions. This baseline uncertainty is associated with the randomness in the time series profile of the wave field caused by the random nature of the wave phases.

This Monte Carlo simulation has only been conducted on one WEC design, one seastate bin and for a single location. Therefore its relevance to other WEC designs, seastates and locations cannot currently be ascertained. This work presents a robust procedure to determine uncertainty for a single seastate bin and demonstrates the importance of establishing this uncertainty.

NUMERICAL SIMULATIONS

Wave Energy Converter

The WEC being simulated is a two body axisymmetric point absorber; a high draft spar that moves in 6 degrees of freedom is attached to a low draft float that is limited to move along the spar's central axes [1–3]. In the simulations, the power is recovered from the relative motion of the float and the spar, using a viscous damper. The WEC schematic is presented in Figure 1.

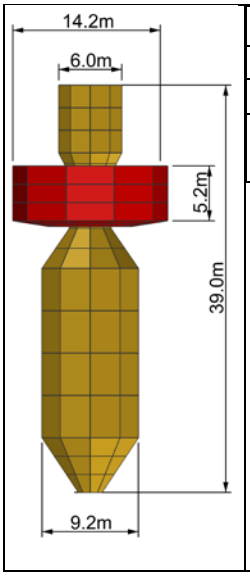

Property	Value
Mass Spar	566 000 kg
Mass Float	201 000 kg
PTO damping	1625000 Ns/m

FIGURE 1. A SCHMATIC OF THE WEC: ITS DIMENSIONS AND SIMULATION PARAMETERS.

The time domain numerical simulations includes: the forcing from the waves and environment (winds and currents), tidal water depth variations, viscous damping, internal forces from the PTO, buoyancy and the reactions of the mooring lines. The simulation platform used is ProteusDS[1,4–6].

As the WEC is small relative to the wavelength, the force from the waves and the environment is calculated as if the WEC was hydrodynamically invisible. The pressure of the combined wave and current field is calculated for each submerged panel on the bodies mesh and summated to provide the total wave forcing. Similarly the pressure from the wind on the dry panels is calculated. The panels used in the calculation are visible in Figure 1.

Viscous drag coefficients are approximations that aim to incorporate viscous fluid flow phenomena that are known to be Reynolds number and KC number dependent. However, when adding viscous drag for a complex geometry, there is great uncertainty is the parameter selection and the drag coefficients are typically obtained from experimental results or from constitute shapes' experimental or analytical results. In this work the results of [7–9], are used to construct estimates of the drag coefficients which are presented in Table 1.

The moorings were originally simulated as three long studlink chains, equidistance apart, connected at the center of buoyancy of the spar. Due to the high computational time required to simulate this mooring, the mooring was simplified to a combination of vertical and horizontal spring-mass-damper assemblies, and a rotational spring-mass-damper system that act to oppose motions. If the spar translated horizontally more than 10 m additional high forces are applied, the equivalent of the moorings lines becoming taut.

Radiation effects are not included due to their relatively small size compared to the viscous drag loading and to reduce computational costs.

Wave and environmental loading

WEC power production estimates are generally based on numerical studies which parameterize and idealize the environmental conditions for individual bins within the resource histogram (See Figure 2). It is commonly accepted practice to simulate the device in wave conditions direction, current speed and direction, and tidal height [10–12] .

The West Coast Wave Initiative at the University of Victoria maintains a series of wave measurement buoys off the West coast of Vancouver Island, Canada. Data from April 1st, 2013 to March 31st, 2014 provided the most complete year of data and was used for this study. The buoy is deployed at 48°53'N and 125°37'W, in 40 m of water and records a full directional wave spectrum, wind and current data. Tidal height data is available from the nearby tidal station at Ucluelet, BC (approx. 7 km from buoy location).

As shown in Figure 2, the most frequently occurring sea state at Amphitrite Bank is between 1.0 – 1.5 m Hs and 8 – 9 s Te [13].

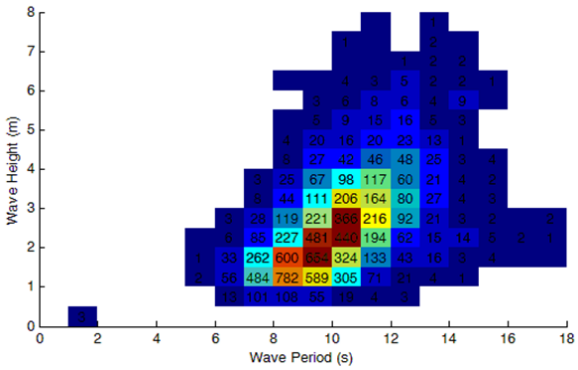

FIGURE 2: HISTOGRAM OF WAVE CONDITIONS AT AMPHITRITE BANK, BC, CANADA.

In addition to the Hs and Te parameters, the following IEC-recommended [14] and commonly used wave parameters were extracted: JONSWAP 'peakiness' parameter (gamma) [15], the primary wave energy direction, wind speed and direction, current speed and direction; and tidal variation.

For each of the parameters a probability distribution function (PDF) was fitted to the datasets determined through minimization of the Bayesian Information Criterion (BIC) values to provide a stochastic input method to quantify all possible combinations of wave, wind, current and tidal conditions; within the 1.25 m Hs and 8.5 s Te bin. All variables were treated independently within this single bin. A sample of the current speed PDF is presented in . Note that some parameters featured double-peaked PDF's and required overlapping distributions to best match the empirical data.

Numerical Simulations: Monte Carlo Approach

In order to quantify and discretize the effects of each variable, this study uses a Monte Carlo approach. The variables included, along with their mean, minimum, maximum or mean ±3σ (as appropriate) and the type of distribution are presented in Table 1. For each simulation, a value is randomly chosen for each independent variable based on the presented distributions.

To enable the Monte Carlo experiment and aid in the understanding of each variables' influence on final WEC power uncertainty, a large number of runs are required. Therefore, the WEC simulation

TABLE 1. THE VARIABLES TESTED AND THEIR STATISTICAL PROPERTIES

	Variable	Unit	Mean	Min or μ-3σ	Max or μ+3σ	Distribution
Wave Seastate	Hs	m	1.25	1.0	1.5	Uniform
	Te	s	8.5	8.0	9.0	Uniform
	Gamma	-	1.74	1	7	Generalized Pareto
	Wave Direction	Deg	79.4	-180	180	T location-scale
Environmental	Current speed	m/s	0.247	0	0.715	Gamma probability
	Current Direction	Deg	45*	-180	180	Double peaked normal **
	Current Direction 1	Deg	-63	-180	180	Normal with 0.44 weighting
	Current Direction 2	Deg	132	-180	180	Normal with 0.56 weighting
	Wind Speed	m/s	4.8	0	13.8	Weibull
	Wind Direction	Deg	5.8*	-180	180	Double peaked normal **
	Wind Direction 1	Deg	-78	-180	180	Normal with 0.59 weighting
	Wind Direction 2	Deg	98	-180	180	Normal with 0.41 weighting
	Tidal height***	m	2.1	-0.26	4.46	Normal
Set up	Frequency bins	-	14****	5*****	23	Normal
	Directional bins	-	20****	5*****	35	Normal
Viscous Drag	Horizontal spar drag	-	0.5	0.125	0.875	Normal
	Vertical spar drag	-	1	0.25	1.75	Normal
	Horizontal float drag	-	1	0.25	1.75	Normal
	Vertical float drag	-	1	0.25	1.75	Normal

* Although this is the mean value, it has a relatively low probability due to the nature of the combined normal distribution. ** A linear combination of the two following normal distributions with weights as stated. *** From a LLWLT (lower low water, large tide) **** Integer units ***** The product of the number of frequency and directional bins is always greater than 100.

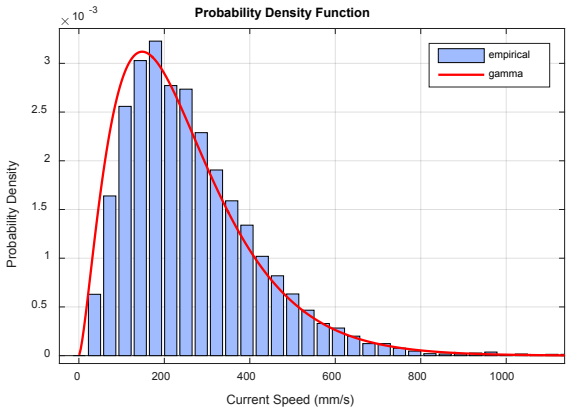

FIGURE 3: PDF OF CURRENT SPEED

model needs to be computational quick while still remaining accurate enough to provide value. The Monte Carlo simulation consisted of 12017 separate simulations, with the simulations lasting 25 min and the final 20 min of the simulation data was used to calculate the mean power, in accordance with [10]. The ProteusDS simulation typically ran at a ~3:1 (simulation time: real time), therefore multi-core high powered computing was required to reach the required number of individual simulations. On a single core machine, this Monte Carlo experiment would take over 600 days.

RESULTS AND DISCUSSIONS

Monte Carlo Simulation results

To ensure that the Monte Carlo experiment has performed sufficient simulations, the running mean and the running standard deviation of the mean power of each individual simulation was recorded and presented in Figure 4. These parameters fluctuations are low after 12000 simulation runs.

The PDF of the mean normalized power recovered is presented in Figure 5. The closest fit to this data was an inverse Gaussian fit, although this does not represent the data well, showing there are multiple factors influencing the variation in mean power.

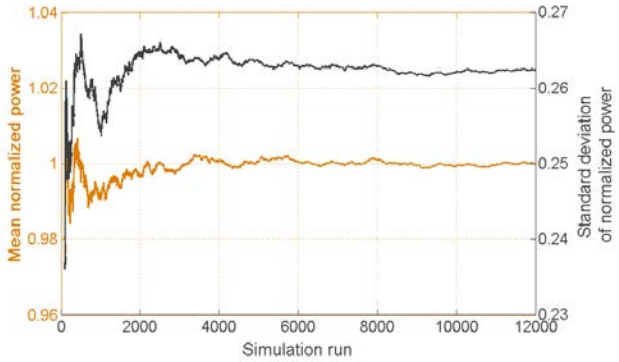

FIGURE 4. THE CONVERGENCE OF THE RUNNING MEAN AND STANDARD DEVIATION OF THE POWER

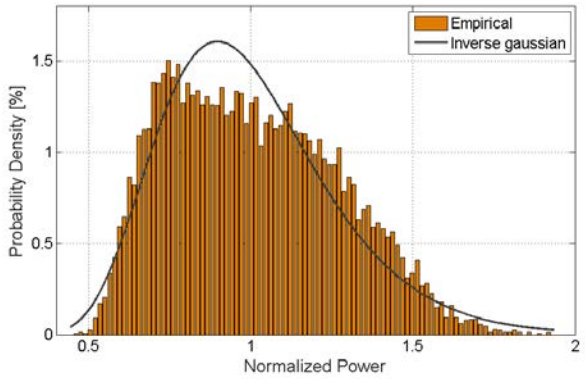

FIGURE 5. THE PDF OF THE NORMALIZED POWER

Detrending the simulation data

Statistical trends in the mean power data were systematically extracted for each variable. The difference in the direction of pairs of the wind, waves and current variables were considered rather than their absolute directions.

The largest absolute correlation coefficients between the normalized power and each variable were used to determine the data detrending order. The linear trendlines were determined using *Matlab's curve fitting toolbox*, with the influence of the outliers reduced by implementing a bisquare robust fit. The normalized power dataset was sequentially detrended by removing trends quantified by the highest correlating variables, and the repeating the process until no further improvements could be made. Note that several variables occurred multiple times, resulting in a cubic Hs and quadratic current magnitude dependence.

In order to visually display the uncertainties associated with each variable, the trendlines for the 8 dominant variables are presented in Figure 6. Each trendline is also multiplied by each simulation run's detrended mean power and presented as dots in the Figure. All the variables increased the uncertainty with quantifiable trends, with the exceptions of the relative angle between the wind and current, and the number of directional segments (and only a very small trend for the number of frequency bins – see Table 2).

Contribution from the different variables

The standard deviation of the recovered normalized mean power for the uncertainty and each of the different variables based on their trendlines is presented in Table 2. The trendlines associated with Hs are a large proportion of the overall variation of the mean power recovered, however the range of Hs (1.0 m to 1.5 m) is large compared to its mean value (1.25 m) and therefore it is postulated that for higher Hs values, the influence of where Hs falls within the bin would be lower (and conversely for lower Hs it would have a greater influence).

The environmental factors have been based on a specific location in the West Coast of Canada. Compared to other locations, were for example the tidal range or currents could be notable larger, or the directions of the waves, wind and currents are not affected by the NW sloped landmass, different results would be expected, that could lead to a different trendline and / or a higher order trendline for these factors.

TABLE 2. THE STANDARD DEVIATION THAT ORIGINATES FROM EACH VARIABLE

Variable	STD from this variable [%]
Hs	15.1
Te	3.59
|∠Wave - ∠Current|	1.25
Gamma	0.201
Current magnitude	0.165
Vertical Float Drag	0.186
Vertical Spar Drag	0.179
Horizontal Float Drag	0.129
|∠Wave - ∠Wind|	0.069
Tidal height	0.033
Horizontal Spar Drag	0.021
Wind magnitude	0.002
Number of frequency bins	0.001
Total from variables	21.0
Total	26.3

Phase uncertainty

The PDF of the normalized and detrended power is presented in Figure 7, alongside the best fit T-location scale distribution, with a mean of 1, a scale parameter of 0.046 and a shape parameter of 8.56; which closely matched the distribution. This PDF is distinctly different to that of Figure 5 which featured the normalized mean power without any detrending.

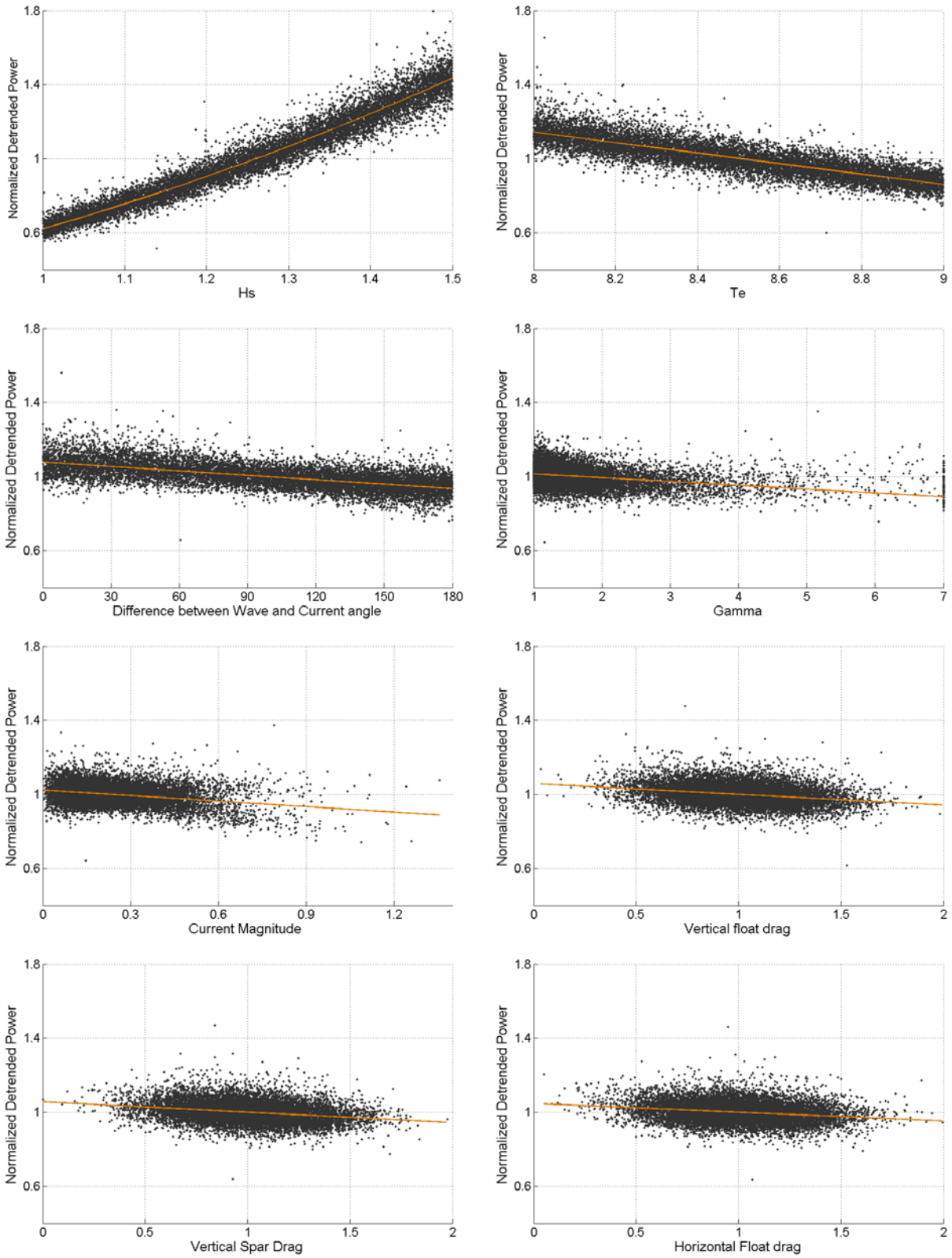

FIGURE 6. THE NORMALIZED DETRENDED POWER AGAINST THE VARIABLE

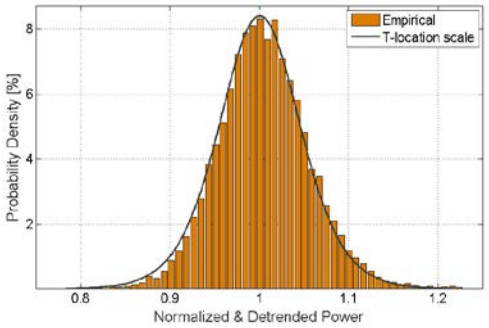

FIGURE 7. THE PDF FOR THE DETRENDED POWER AND A FITTED T-LOCATION SCALE.

For the same spectral sea state there are variations in the time domain wave distribution due to the different wave phases and the exact directions and frequencies for each of the regular waves that are summated together to form the seastate. These phase, directional and frequency differences lead to differences in power recovered, which has no discernable trend due to the number of variations that are possible and will always be present for any identical spectral seastate in the ocean. This can be considered to be the inherent variability for a known situation and is referred to as *phase uncertainty* henceforth.

CONCLUSIONS

A large Monte Carlo approach has been used to quantify and discretize the effect of environmental, numerical and seastate variable on mean WEC power production. The simulations have shown that the variations in the mean power recovered, for a single seastate, can vary with a standard deviation of 26% of the mean power, of which 19% can be attributed to Hs and Te variation within the seastate Hs-Te bin and 5% from the inherent phase uncertainty of the wave climate.

ACKNOWLEDGEMENTS

This work was funded by Natural Resources Canada, the Natural Sciences and Research Council of Canada and the Pacific Institute of Climate Solutions.

REFERENCES

[1] Bailey, H., Ortiz, J., Robertson, B., Buckham, B., and Nicoll, R., 2014, "A Methodology for Wave-To-Wire WEC simulations," Marine Renewable Energy Technology Symposium (METS2014), Seattle, WA.

[2] Beatty, S. J., Buckham, B. J., and Wild, P., 2013, "Experimental comparison of self-reacting point absorber WEC designs," European Wave and Tidal Energy Conference, (EWTEC 2013), Aalborg, Denmark.

[3] Weber, J., Mouwen, F., Parish, A., and Robertson, D., 2009, "Wavebob – Research & Development Network and Tools in the Context of Systems Engineering," 8th European Wave and Tidal Energy Conference (EWTEC 2008), Uppsala, Sweden.

[4] Combourieu, A., Lawson, M., Babarit, A., Ruehl, K., Roy, A., Costello, R., Weywada, P. L., and Bailey, H., 2015, "WEC3 : Wave Energy Converter Code Comparison Project," Proceedings of the 11th European Wave and Tidal Conference (EWTEC 2015), Nantes, France.

[5] Garcia-Rosa, P. B., Costello, R., Dias, F., and Ringwood, J. V, 2015, "Hydrodynamic Modelling Competition - Overview and Approaches," 34th International Conference on Ocean, Offshore and Arctic Engineering (ASME 2015), St. John's, Newfoundland, Canada.

[6] Nicoll, R. S., Wood, C. F., and Roy, A. R., 2012, "Comparison of Physical Model Tests With a Time Domain Simulation Model of a Wave Energy Converter," ASME 2012 31st International Conference on Ocean, Offshore and Arctic Engineering., Rio de Janeiro, Brazil.

[7] Babarit, A., Hals, J., Muliawan, M. J., Kurniawan, A., Moan, T., and Krokstad, J., 2012, "Numerical benchmarking study of a selection of wave energy converters," Renew. Energy, 41, pp. 44–63.

[8] Sarpkaya, T., 1986, "Force on a circular cylinder in viscous oscillatory flow at low Keulegan—Carpenter numbers," J. Fluid Mech., 165, p. 61.

[9] Beatty, S. J., Roy, A., Bubbar, K., Ortiz, J., Buckham, B. J., Wild, P., Stienke, D., and Nicoll, R., 2015, "Experimental and numerical simulations of moored self-reacting point absorber wave energy converters," Proceedings of the International Offshore and Polar Engineering Conference (ISOPE 2015), Kona, Hawaii Big Island.

[10] International Electrotechnical Commission T C 114, 2014, IEC TS 62600-100 Technical Specification - Part 100: Electricity producting wave energy converters - Power performance assessment.

[11] Carballo, R., and Iglesias, G., 2012, "A methodology to determine the power performance of wave energy converters at a particular coastal location," Energy Convers. Manag., 61, pp. 8–18.

[12] Robertson, B., Clancy, D., Bailey, H., and Buckham, B., 2015, "Improved Energy Production Estimates from Wave Energy Converters through Spectral Partitioning of Wave Conditions," International Society of Offshore and Polar Engineers (ISOPE 2015).

[13] Robertson, B., Hiles, C. E., Luczko, E., and Buckham, B. J., 2016, "Quantifying the Wave Power and Wave Energy Converter Array Production Potential," Int. J. Mar. Energy.

[14] IEC, 2012, TC114: Marine energy - Wave, tidal and other water current converters - Part 100: Electricity producing wave energy converters - Power performance assessment, IEC/TS 62600-100 Ed. 1.0.

[15] Robertson, B., Bailey, H., Clancy, D., Ortiz, J., and Buckham, B., 2016, "Influence of wave resource assessment methodology on wave energy production estimates," Renew. Energy, 86, pp. 1145–1160.